Catalysis Science & Technology

ROYAL SOCIETY OF CHEMISTRY

PAPER

View Article Online
View Journal | View Issue



Cite this: *Catal. Sci. Technol.*, 2025, 15, 5886

# Scavenging of photogenerated holes in $TiO_2$-based catalysts uniquely controls pollutant degradation and hydrogen formation under UVA or visible irradiation

Nelson Rutajoga, Valerie Velez and Juan C. Scaiano *

The use of heterogeneous photocatalysts to degrade hard-to-remove pharmaceuticals from polluted water offers a promising approach for efficient water treatment. These contaminants, commonly found in rivers and lakes, can be traced back to wastewater effluents containing harmful chemical species, including endocrine disruptors. Our research provides valuable insights into the functioning of known $TiO_2$-based photocatalysts as well as novel materials designed to expand the catalyst's absorption range into the visible region. This includes $TiO_2$, Pd@$TiO_2$, Cu@$TiO_2$, and Au@$TiO_2$. Among the emerging photocatalysts, black $TiO_2$ (b-$TiO_2$) was selected as the starting point, and subsequently decorated with metal nanoparticles to produce Pd@b-$TiO_2$, Cu@b-$TiO_2$, and Au@b-$TiO_2$. Mechanistic findings reveal that hole trapping consistently emerges as the yield-determining step, with electron scavenging following closely behind. Consequently, oxygen or proton trapping of electrons has no significant impact on the overall efficiency of removal of pollutants. Additionally, we present a methodology for screening the capability of newly designed materials to photodegrade pollutants by measuring the output of $H_2$. This eliminates the need for series of experimental trials specific to each target pollutant; thereby, streamlining conventional processes upheld in this field. Each of these materials was first tested for their hydrogen generating ability under UV and visible light using methanol and formic acid as sacrificial electron donors, as well as estradiol, ibuprofen, and acetaminophen. Following this, ibuprofen was selected for extended studies where it would be photooxidized and/or release $H_2$ gas as a by-product that is readily detectable using gas chromatography.

Received 15th June 2025,
Accepted 20th August 2025

DOI: 10.1039/d5cy00720h

rsc.li/catalysis



## Introduction

The current research landscape is dominated by an intense focus on synthesizing novel heterogeneous catalysts. These catalysts have applications in both the synthesis of organic compounds, particularly pharmaceuticals, and the degradation of organic pollutants, including pharmaceuticals.[1,2] In the context of environmental remediation, photocatalysts can be utilized through oxidative pathways that lead to mineralization, or under anaerobic conditions that simultaneously degrade pollutants and generate hydrogen.[3] In this work, we have developed $TiO_2$-based photocatalysts that possess the unique ability to perform both functions, utilizing either ultraviolet or visible light.

In recent decades, there has been a growing interest in removing various types of environmental pollutants from natural bodies of water, or to produce drinking water. Among the chemical species that contaminate waterways, pharmaceuticals have garnered particular attention due to their challenging removal. These pollutants, particularly endocrine disruptors, interfere with the development of species exposed to these hazardous compounds.[4] Titanium dioxide ($TiO_2$), a semiconductor that has been extensively studied and modified for degrading contaminants using light-driven heterogeneous catalysis, has a limited absorption range in the ultraviolet region. This is because $TiO_2$ has a wide band gap, approximately 3.1 eV for anatase. To address this limitation, metal doping and decorating are common methods to extend the photoactivity of $TiO_2$-based catalysts into the visible region.[5–7] Additionally, modifying $TiO_2$ through reductive treatment has emerged as a useful technique to broaden the absorption range of the metal oxide, usually attributed $Ti^{3+}$ and oxygen vacancies as active sites which alter the bulk properties of the catalyst.[8–10] The reactivity of black-$TiO_2$ remains a subject of active research and conflicting interpretations.[11]

*Department of Chemistry and Biomolecular Sciences, University of Ottawa, 10 Marie Curie, Ottawa, ON K1N 6N5, Canada. E-mail: jscaiano@uottawa.ca*

In this work we have decorated $TiO_2$ with Pd, Cu and Au, as all three have been shown to improve its photocatalytic activity,[12–14] and their performance in the presence of sacrificial electron donors (SED) usually exceeds by about two orders of magnitude that in the absence of SED (true water splitting).[15]

Beyond metal decoration, we have also examined novel decorated black $TiO_2$ catalysts; these blackened photocatalysts possess reduced $TiO_2$ sites with a reduced bandgap.[16]

The ability of photocatalysts to degrade organic matter has frequently been tested using organic dyes, for example methylene blue.[17–19] Our choice in recent contributions has usually been crocin, as many of our catalysts contain glass fibers and methylene blue has a tendency to bind to glassy materials.[9,20] The frequent preference for surrogate materials, rather than actual contaminants, reflects that each contaminant requires the time consuming development and validation of analytical methods and materials for each substrate.

We propose a rapid screening method for potential catalysts and their spectral responses by assessing their ability to generate hydrogen from various contaminants. This approach has been suggested for hydrogen generation from contaminants,[3] but has never been evaluated or developed as a tool to test environmentally useful catalysts. While $H_2$ generation provides no information on the detailed catalytic pathway, it provides compelling proof of the photocatalyst's competence in the oxidation of contaminants. Thus, our proposal involves the use of photocatalytic $H_2$ generation as a rapid screening strategy that will allow us to select and prioritize those materials where the investment in a full characterization of the catalytic degradation of contaminants is justified.

An important conclusion that emerges from our work is that the photocatalytic activity under oxidative or anaerobic conditions, whether in the visible or ultraviolet region and regardless of the dopant or absence of a dopant, is solely determined by the initial hole trapping event by the organic molecule.

## Results and discussion

### Materials

Two common SED were utilized in early testing, methanol and formic acid, both well established as easily oxidizable in previous research.[15] In addition, three common pharmaceuticals were also tested, estradiol, ibuprofen and acetaminophen; their structures are shown in Scheme 1.

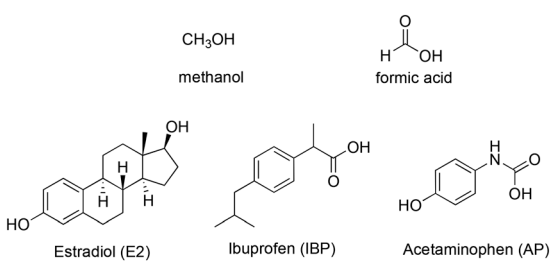


Scheme 1 Molecules studied in this work.

All the catalysts are based on P25, a common $TiO_2$ material, consisting predominantly of anatase (about 84%), with rutile as the balance. Thermal treatments required for the synthesis of the eight catalysts used were limited to temperatures below 400 °C in order to prevent the conversion of anatase to the thermodynamically favored rutile. Table 1 shows the materials used and the corresponding nomenclature; we note that Cu-containing materials will be partially oxidized and contain significant levels of Cu(II).[21] Further synthetic details are available in the SI, although we note that some of the catalysts (earlier batches) were included in other publications.[15,21,22]

Light absorption plays a crucial role in our work, making it essential to understand the spectroscopy of the materials listed in Table 1. The diffuse reflectance of these catalysts is depicted in Fig. 1. The Kubelka–Munk analysis generates a reflectance function, $F(R)$.[23,24] For instance, once blackened, $TiO_2$ exhibits values of $F(R)$ exceeding 6, indicating that at least 94% of the light is absorbed within the visible region. Conversely, values exceeding 1.5, achieved with gold and palladium, signify that over 80% of the light is absorbed. For instance, in panel C, blackening of Pd@$TiO_2$ leads to an increase in light absorption from approximately 85% to over 94%.

While the photodegradation of pollutants typically relies on pathways involving reactive oxygen species, the possibility of utilizing anaerobic pathways that lead to hydrogen evolution presents an intriguing alternative.[3] Both processes involve the scavenging of electrons from the $TiO_2$ conduction band. However, our studies indicate that the entire degradation process is actually controlled by hole scavenging, regardless of the excitation wavelength or the decoration of the semiconductor nanostructure.

### Experiments with acetonitrile as co-solvent

The catalysts in Table 1 were tested using UVA light centered at 370 nm and visible light (400–700 nm). Initially, experiments with pharmaceuticals were conducted in a 20% acetonitrile solution in water to address solubility challenges. However, the photogenerated hole in $TiO_2$ is so highly electrophilic that even acetonitrile can act as a sacrificial electron donor.[25] Consequently, a substantial portion of the hydrogen produced in this solvent is attributed to acetonitrile rather than the pharmaceuticals depicted in Scheme 1. Nevertheless, these preliminary findings reveal some intriguing observations, and a comprehensive summary of the results is provided in the SI. Most of the experiments described herein were conducted in water, and the concentrations were adjusted to ensure solubility. In retrospect, while these aqueous concentrations are higher than typical contaminant levels, they are closer to environmental levels compared to those

**Table 1** Catalysts used for hydrogen generating experiments[a]

| Metal NP decoration | Catalysts on $TiO_2$ | Catalysts on black $TiO_2$ | % metal content |
|---|---|---|---|
| None | $TiO_2$ (P25) | b-$TiO_2$ | 0 |
| Palladium | Pd@$TiO_2$ | Pd@b-$TiO_2$ | 1.5 |
| Copper | Cu@$TiO_2$ | Cu@b-$TiO_2$ | 2.0 |
| Gold | Au@$TiO_2$ | Au@b-$TiO_2$ | 3.0 |

[a] Photographs of some of the materials are available in the SI.

that could be achieved when acetonitrile serves as a co-solvent.

The data that follows concentrates on the pharmaceuticals tested. In the SI we include figures that show the efficiency of these catalysts producing hydrogen from SED, with performance in the order HCOOH > $CH_3OH$ > $CH_3CN$. The catalysts are active both in the UV and visible regions.

The use of acetonitrile as a co-solvent proved beneficial in determining the relative reactivity of the three pharmaceuticals under investigation. Solubility concerns were eliminated in this solvent, and all three compounds exhibited substantial photodegradation within an hour when exposed to either ultraviolet or visible light, as depicted in Fig. 2. We note that in all experiments that follow the irradiance was 177 W $m^{-2}$ in the UVA region and 432 W $m^{-2}$ in the visible region, corresponding to a ratio of 2.44 (vis/UVA); detailed LED spectra are available in the SI. If we prefer to have this ratio in terms of number of photons (einsteins) instead of watts, this ratio is ~3.6 using 370 nm for UVA and 550 nm for visible light; note that 550 nm is the center of the visible spectrum.

Fig. 2 illustrates that E2 is the least reactive molecule, with 1680 molecules of $H_2$ generated for every E2 consumed. In contrast, the ratios for IBP and AP are 1070 and 137, respectively. In this solvent, most of the hydrogen is generated from the acetonitrile used as co-solvent. Among the pharmaceuticals tested, acetaminophen is the easiest molecule to degrade. Here the modest reactivity of acetonitrile facilitates this comparison. Note that given the molarity and concentration of acetonitrile, its concentration in the samples is 38 000 larger than that of the target pharmaceuticals; on a molar basis the latter as far more reactive than acetonitrile, as anticipated.

A remarkable feature of Fig. 2 is that while different molecules have different reactivity, for each molecule the points fit in an excellent line regardless of the light used, the metal decorating $TiO_2$, or whether the $TiO_2$ has been reductively darkened or not. While Fig. 2 only identifies the type of light, full details of the catalyst used and conditions are available in Tables S1 and S2 in the SI. We will return to discuss this observation after we present our results when pure water is the solvent.

To address the potential for these catalytic materials to be used in a more complex systems, simulating current real-world conditions in bodies of water, experiments were conducted combining the three aforementioned organic pollutants, AP, IBP, and E2 in addition to L-ascorbic acid, AA, (0.1 mM) acting as a potent hole and radical scavenger. Although vitamin C is not a contaminant of concern in lakes and rivers, its ability to scavenge photo-generated holes and

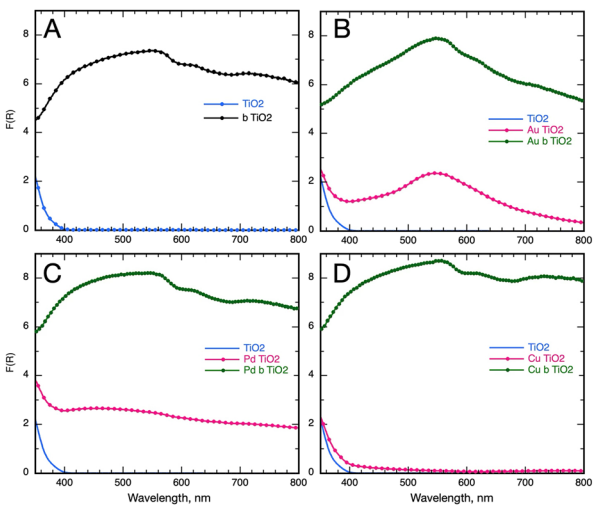


**Fig. 1** Diffuse reflectance spectra for the catalysts in Table 1. Panels A, B, C, and D show the spectra for b-$TiO_2$, Au@$TiO_2$ with Au@b-$TiO_2$, Pd@$TiO_2$ with Pd@b-$TiO_2$, and Cu@$TiO_2$ with Cu@b-$TiO_2$, respectively. The spectrum for pristine $TiO_2$ (blue) has been included in all panels.

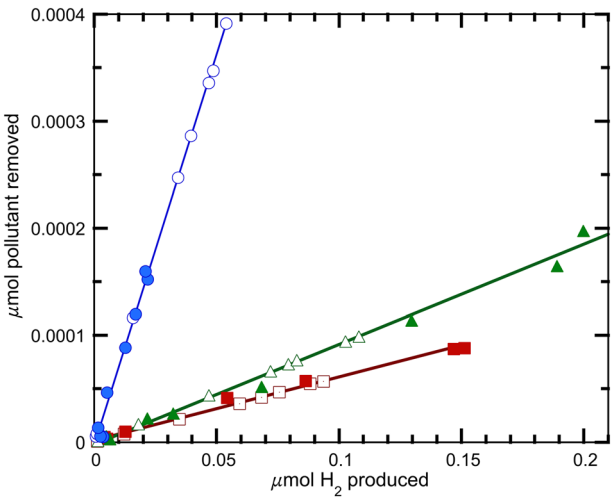


**Fig. 2** Amount of organic compound removed shown against the moles of hydrogen produced for 0.1 mM solutions on 20% acetonitrile : water (v/v). Filled points are for UV data and open points for visible data: red squares for E2, green triangles for IBP and blue circles for AP.

 

free radicals has been demonstrated in prior studies[26,27] and makes it ideal to act as a surrogate species for other prevalent hole and radical scavengers that may be naturally present in the environment such as humic acid.[28] The results presented in Fig. 3 indicate that the presence of additional pollutants does not substantially diminish the activity of the catalysts. When combining AP, IBP, and E2 (all at a concentration of 0.1 mM), there is only a slight reduction in the rate of removal compared to the results depicted in Fig. 2. This suggests that, when combined, these pollutants are degraded independently of each other. Notably, the irradiation time for the pollutant mixture was one hour, while when the pollutants were treated separately, the irradiation time was one hour for each pollutant. The degradation achieved when the pollutants were combined was approximately 90% of the degradation achieved when the pollutants were treated separately. When AA, a hole scavenger, was added to the three-contaminant system, there was a noticeable decrease in the performance of the catalysts, resulting in a performance of around 50%. However, AA effectively scavenges reactive holes, decreasing the oxidation of the pollutants. Despite this reduction in performance, the catalysts remain effective in degrading all three organic targets under UVA and visible light. These studies were performed in 20% acetonitrile : water to eliminate solubility issues.

Fig. 3 depicts two radar plots highlighting the performance of all 8 catalysts under UVA (panel A of Fig 3) or visible (Panel B of Fig. 3) irradiation with the target pollutant being IBP. These plots are paired with averages of the consumed amount of IBP in conditions where the contaminant is present in an aqueous medium on its own, mixed with E2 and AP, as well as mixed with E2, AP, and AA (all at 0.1 mM).

An exploratory study for Cu@$TiO_2$ of the relative effect of mixing and vitamin C addition on the relative response of different pollutants suggests a virtually identical response as measured by degradation ratios for each pollutant (Fig. S17). While this graphic underscores the performance of Cu@$TiO_2$, it can be noted that a similar study can be examined for all other catalysts as well when using the data shown in Table S6.

In order to perform further detailed studies we selected ibuprofen as the choice material; we note that E2 had been studied at least with pristine and blackened $TiO_2$ in a recent contribution.[9]

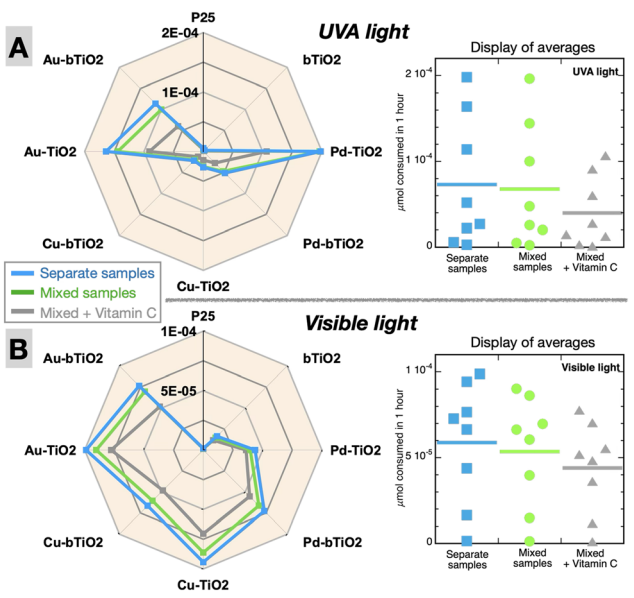


Fig. 3 Radar plots showing the consumption of IBP for all 8 catalysts under UVA or visible light and in different colors when irradiated alone (blue) or in the presence of AP and E2 as components of the same mixture (green). The gray data shows the effect of adding 0.1 mM vitamin C. The plots on the right show the distribution of IBP consumption for the three conditions, while the horizontal bar shows the average. The irradiances used for UVA and visible light are different: UVA (177 W $m^{-2}$) and visible light (432 W $m^{-2}$). Panels A and B denote trials conducted under UVA or visible irradiation respectively.

## Studies of ibuprofen in pure water

Reported solubilities of IBP in water at room temperature range from 0.06 to 0.2 mM,[29,30] making our standard concentration of 0.1 mM close to the solubility limit, however, it proved adequate for all the studies that follow. Fig. 4 shows the results for 1 hour exposure under air or argon and in all cases the letter 'b' before $TiO_2$ indicated that the support is black $TiO_2$.

The data for visible light has been divided by 2.44 (*vide supra*) so that UVA and visible data are referred to an irradiance of 177 W $m^{-2}$. No hydrogen was detected for exposures under air.

Several features of Fig. 4 are immediately evident. Firstly, the amount of hydrogen produced is significantly higher than the ibuprofen consumed. Secondly, the amount of ibuprofen consumed remains the same regardless of whether it is consumed under air or argon. Catalysts containing Au or

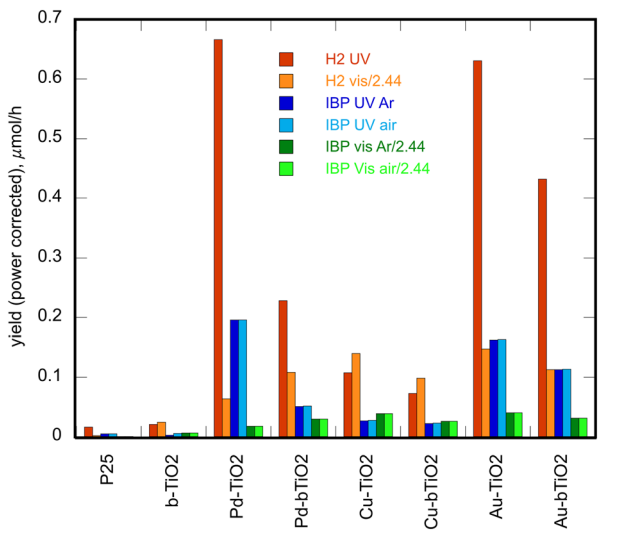


Fig. 4 Yield of hydrogen, or consumption of ibuprofen after 1 hour irradiation of a 0.1 mM solution of ibuprofen in water. The units are μmol per hour and the visible irradiation data have been divided by 2.44 to correct for the stronger visible light source. In this way all results are referred to a nominal irradiance of 177 W $m^{-2}$.

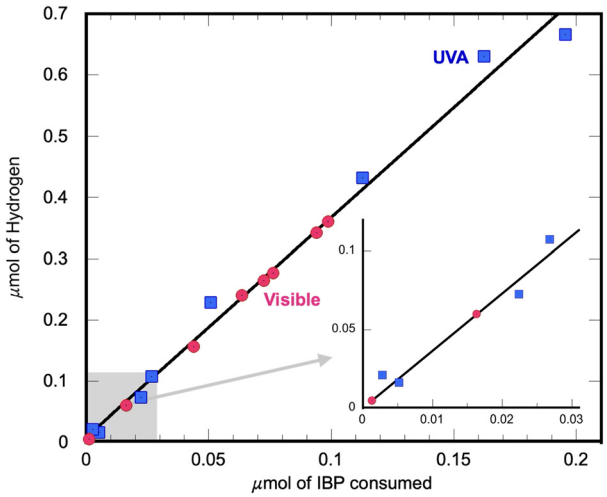


**Fig. 5** Yield of hydrogen after 1 hour irradiation of aqueous 0.1 mM IBP with UVA (177 W $m^{-2}$) or visible light (432 W $m^{-2}$). All eight catalysts in Table 1 were tested. The inset (bottom right) is an expansion of the shaded region, showing the even the least efficient catalysts obey the same correlation. See Table S5.

Pd perform exceptionally well under UVA light; however, under visible light, copper, a more affordable material, performs quite well and could be a suitable choice if the usage or elements at risk of depletion is a concern.

While Fig. 4 can be a helpful guide for selecting catalysts, it fails to reveal the fascinating mechanistic connections between hydrogen generation and ibuprofen degradation. Notably, the hydrogen yield in the presence and absence of ibuprofen only shows a reasonable correlation when using visible light, but not so with UVA light, Fig. S10. Yet, Fig. 5 presents an excellent correlation between hydrogen yields and ibuprofen consumption for all catalysts, regardless of whether UVA or visible light is used. The slope of these graphs indicates that approximately 3.6 molecules of hydrogen are produced regardless of all other experimental parameters and the type of light employed.

As previously mentioned, no hydrogen was produced when the samples were exposed to air. Additionally, we compared the rate of ibuprofen consumption under argon and under air. This comparison yielded an excellent correlation, as evident in Fig. 6, which demonstrates that the atmosphere (air *versus* argon) has no impact on the rate of ibuprofen consumption, irrespective of all other experimental parameters and the type of light used.

The results in Fig. 5 and 6 support the idea that the catalysis observed is solely controlled by the rate of hole scavenging by the organic molecule, ibuprofen in our examples. Further, the fact that ~3.6 molecules of hydrogen are produced for each ibuprofen molecule consumed suggests that ibuprofen is well on its way to complete mineralization. Processes that involve trapping the electrons generated in the conduction band do not seem to affect the overall kinetics although they must be part of a cascade of oxidative processes that generate hydrogen or the reactive oxygen species (ROS) that degrade ibuprofen through various effective pathways. Moreover, the observation that 3.6 molecules of hydrogen are produced while a significant portion of IBP remains in the sample, suggests that the initial degradation products are more readily oxidized compared to IBP itself.

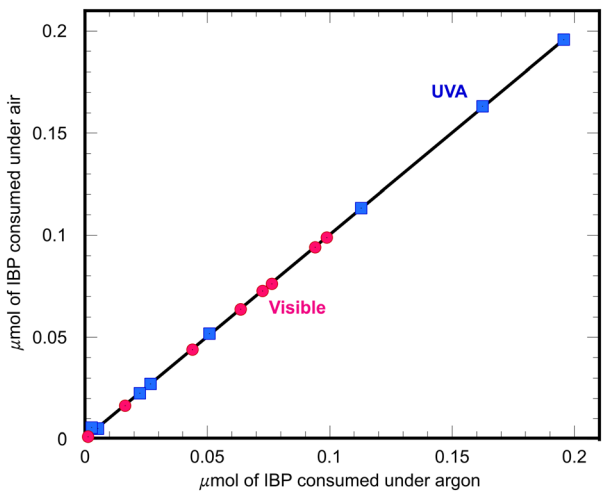


**Fig. 6** Ibuprofen consumed after 1 hour irradiation of aqueous 0.1 mM IBP with UVA (177 W $m^{-2}$) or visible light (432 W $m^{-2}$). Data under air plotted against data under argon. All eight catalysts in Table 1 were tested.

## Mechanism

The mechanism of reaction proposed is shown in Scheme 2, where A shows the UVA mechanism with the classic hole scavenging by the substrate followed by oxidation of the radical accompanied by $H_2$ evolution under anaerobic conditions. The mechanism in B starts with excitation of the metal decoration followed by the same processes as in A, but with no direct involvement of the valence band of $TiO_2$. The

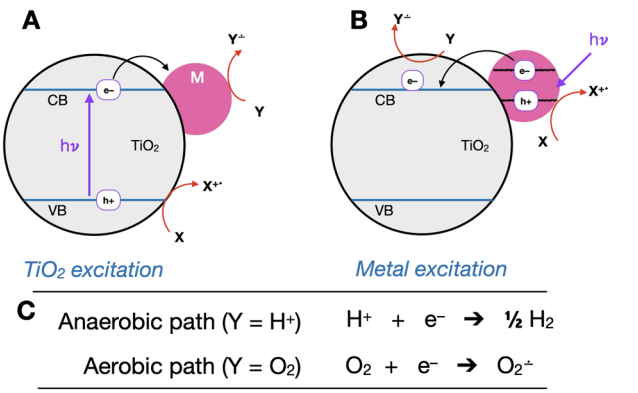


**Scheme 2** Schematic representation pathways following M@$TiO_2$ excitation. In A UV excitation leads to predominant absorption by $TiO_2$ followed by electron transfer to M, while on B visible excitation is largely absorbed by M, following electron transfer that populates the conduction band of $TiO_2$. For black $TiO_2$, both M and the color centres in $TiO_2$ can be active chromophores. In both cases hole scavenging can involve an SED or a pharmaceutical, while electron scavenging is different under aerobic or anaerobic conditions (C).

mechanism has been proposed by Gomes Silva *et al.* for reaction of Au@$TiO_2$ with EDTA as SED,[31] and has also been described as hot electron injection.[32] The interaction of the hole in the metal with the $TiO_2$ band structure is intricate and still a subject of ongoing research. The intense plasmon fields near the plasmonic nanoparticles can induce charge shifts within the host structure, which may actively participate in hole scavenging reactions. Regardless, it is evident that $TiO_2$ goes beyond being a mere support; it actively contributes to the overall process when visible light excites the metal nanoparticle.[32,33]

## Conclusions

Our findings indicate that the yield of pollutant photodegradation is solely determined by the efficiency of hole scavenging. The effectiveness of hole scavenging varies across different materials, and the wavelength of the excitation light also plays a crucial role in this process. It's not surprising that Pd@$TiO_2$ (Fig. 3) performs exceptionally well under UV irradiation. A material of particular interest is Cu@$TiO_2$, which exhibits excellent performance under visible light. Moreover, it is an inexpensive material, relatively abundant, and poses minimal health risks. Once hole scavenging is achieved, conduction band electrons simply follow, leading to the production of hydrogen or reactive oxygen species depending on the availability of oxygen in the medium. Typically, hydrogen yields are 3.6 molecules per ibuprofen degraded, and require that the initial degradation of IBP be followed by products that facilitate additional oxidative degradation. The complex mixture of products resulting from IBP photooxidation has been reported in earlier studies.[34,35]

The recyclability of the photocatalysts examined in this study is crucial when considering their practical use. Fig. S11–S14 illustrate the removal of the target pharmaceutical using our catalysts after three photodegradation cycles. Notably, blackened and decorated $TiO_2$ analogs exhibit excellent recyclability for removing pharmaceuticals. It is noteworthy that Cu-decorated photocatalysts maintain their performance throughout the three cycles, making them suitable greener materials for remediation applications compared to Au or Pd-decorated photocatalysts. Additionally, as depicted in Fig. 3, Cu@$TiO_2$ demonstrates exceptional performance under visible light irradiation.

## Experimental

The light-driven hydrogen generation trials were conducted by suspending 10 mg of catalyst in 4 mL of an aqueous solution containing 1% of a sacrificial donor (methanol or formic acid) or a 0.1 mM concentration of a pharmaceutical pollutant (estradiol, acetaminophen, or ibuprofen). These solutions were prepared in 10 mL borosilicate crimp vials that were purged and sealed under nitrogen. Irradiation was performed with continuous stirring for 60 minutes. Following irradiation, a 1 mL sample of the headspace was collected using a lock syringe and manually injected into the gas chromatograph with a thermal conductivity detector (GC-TCD). The $H_2$ gas was detected at a retention time of 3.9 min (see SI Fig. S7) and quantified using an established calibration curve. In the case of the pharmaceutical solutions, the liquid phase after irradiation was used for HPLC analysis. A 80 : 20 gradient (water/acetonitrile) was used as the mobile phase while maintaining a constant flow rate of 2.5 mL $min^{-1}$. Changes in absorbance were recorded at 280 nm for estradiol and acetaminophen and at 265 nm for ibuprofen experiments.

Additional details, including material characterization are included in the SI.

## Conflicts of interest

There are no conflicts to declare.

## Data availability

Supplementary information is available. See DOI: **https://doi.org/10.1039/D5CY00720H**.

The data supporting this article have been included as part of the SI.

## Acknowledgements

This work was supported by the Natural Sciences and Engineering Research Council of Canada and the Canada Foundation for Innovation.

## Notes and references

1 J. C. Colmenares and R. Luque, Heterogeneous photocatalytic nanomaterials: prospects and challenges in selective transformations of biomass-derived compounds, *Chem. Soc. Rev.*, 2014, **43**, 765–778.
2 S. Rehman, R. Ullah, A. M. Butt and N. D. Gohar, Strategies of making TiO2 and ZnO visible light active, *J. Hazard. Mater.*, 2009, **170**, 560–569.
3 A. E. Lanterna and J. C. Scaiano, Photoinduced Hydrogen Fuel Production and Water Decontamination Technologies. Orthogonal Strategies with a Parallel Future?, *ACS Energy Lett.*, 2017, **2**, 1909–1910.
4 R. Wang, X. Ma, T. Liu, Y. Li, L. Song, S. C. Tjong, L. Cao, W. Wang, Q. Yu and Z. Wang, Degradation aspects of endocrine disrupting chemicals: A review on photocatalytic processes and photocatalysts, *Appl. Catal., A*, 2020, **597**, 117547.
5 K. Sridharan and T. J. Park, Thorn-ball shaped TiO2 nanostructures: Influence of Sn2+ doping on the morphology and enhanced visible light photocatalytic activity, *Appl. Catal., B*, 2013, **134–135**, 174–184.
6 K. Sridharan, E. Jang and T. J. Park, Deformation assisted fabrication of uniform spindle, tube and rod shaped nanoscale 3D TiO2 architectures and their photocatalytic activity, *CrystEngComm*, 2013, **15**, 8241–8245.

7 S. Shenoy and K. Sridharan, A robust photocatalyst using silver quantum clusters grafted in titanium dioxide nanotubes, *Surf. Interfaces*, 2022, **30**, 101941.
8 Y. Wang, C. Feng, M. Zhang, J. Yang and Z. Zhang, Visible light active N-doped TiO2 prepared from different precursors: Origin of the visible light absorption and photoactivity, *Appl. Catal., A*, 2011, **104**, 268–274.
9 M. Yaghmaei, D. R. C. da Silva, N. Rutajoga, S. Currie, Y. Li, M. Vallieres, M. J. Silvero, N. Joshi, B. Wang and J. C. Scaiano, Innovative Black TiO2 Photocatalyst for Effective Water Remediation Under Visible Light Illumination Using Flow Systems, *Catalysts*, 2024, **14**, 775.
10 X. Chen, L. Liu, Z. Liu, M. A. Marcus, W.-C. Wang, N. A. Oyler, M. E. Grass, B. Mao, P.-A. Glans, P. Y. Yu, J. Guo and S. S. Mao, Properties of Disorder-Engineered Black Titanium Dioxide Nanoparticles through Hydrogenation, *Sci. Rep.*, 2013, **3**, 1510.
11 T. S. Rajaraman, S. P. Parikh and V. G. Gandhi, Black TiO2: A review of its properties and conflicting trends, *Chem. Eng. J.*, 2020, **389**, 123918.
12 Q. Fu, T. Wagner, S. Olliges and H.-D. Carstanjen, Metal −Oxide Interfacial Reactions: Encapsulation of Pd on TiO2 (110), *J. Phys. Chem. B*, 2005, **109**, 944–951.
13 B. Gupta, A. A. Melvin, T. Matthews, S. Dash and A. K. Tyagi, TiO2 modification by gold (Au) for photocatalytic hydrogen (H2) production, *Renewable Sustainable Energy Rev.*, 2016, **58**, 1366–1375.
14 L. S. Yoong, F. K. Chong and B. K. Dutta, Development of copper-doped TiO2 photocatalyst for hydrogen production under visible light, *Energy*, 2009, **34**, 1652–1661.
15 A. S. Hainer, J. S. Hodgins, V. Sandre, M. Vallieres, A. E. Lanterna and J. C. Scaiano, Photocatalytic Hydrogen Generation Using Metal-Decorated TiO2: Sacrificial Donors vs True Water Splitting, *ACS Energy Lett.*, 2018, **3**, 542–545.
16 Y. Li, Black Titanium Dioxide: Synthesis, Characterization and Applications, *MSc Thesis*, University of Ottawa, 2021.
17 M. Wongaree, A. Bootwong, S. Choo-in and S. Sato, Photocatalytic reactor design and its application in real wastewater treatment using TiO2 coated on the stainless-steel mesh, *Environ. Sci. Pollut. Res.*, 2022, **29**, 46293–46305.
18 J. Oyim, M. Jokazi, J. Mack, E. Amuhaya and T. Nyokong, Indium porphyrin - colloidal activated carbon composites for photocatalytic activity against an organic pollutant and bacteria, *Polyhedron*, 2024, **253**, 116918.
19 H. M. Mousa, J. F. Alenezi, I. M. A. Mohamed, A. S. Yasin, A.-F. M. Hashem and A. Abdal-hay, Synthesis of TiO2@ZnO heterojunction for dye photodegradation and wastewater treatment, *J. Alloys Compd.*, 2021, **886**, 161169.
20 D. R. C. da Silva, S. Mapukata, S. Currie, A. A. Kitos, A. E. Lanterna, T. Nyokong and J. C. Scaiano, Fibrous TiO2 Alternatives for Semiconductor-Based Catalysts for Photocatalytic Water Remediation Involving Organic Contaminants, *ACS Omega*, 2023, **8**, 21585–21593.
21 B. Wang, J. Durantini, J. Nie, A. E. Lanterna and J. C. Scaiano, Heterogeneous Photocatalytic Click Chemistry, *J. Am. Chem. Soc.*, 2016, **138**, 13127–13130.
22 T. A. Gawargy, P. Costa, A. E. Lanterna and J. C. Scaiano, Photochemical benzylic radical arylation promoted by supported Pd nanostructures, *Org. Biomol. Chem.*, 2020, **18**, 6047–6052.
23 G. Kortüm, W. Braun and G. Herzog, Principles and Techniques of Diffuse Reflectance Spectroscopy, *Angew. Chem., Int. Ed. Engl.*, 1963, **2**, 333–404.
24 P. Kubelka, New Contributions to the Optics of Intensely Light-Scattering Materials, *J. Opt. Soc. Am.*, 1948, **38**, 448.
25 A. Hainer, N. Marina, S. Rincon, P. Costa, A. E. Lanterna and J. C. Scaiano, Highly electrophilic titania hole as a versatile and efficient photochemical free radical source, *J. Am. Chem. Soc.*, 2019, **141**, 4531–4535.
26 E. Niki, in *Selected Vitamins, Minerals and Functional Consequences of Maternal Malnutrition*, S. Karger AG, 1991, vol. 64, pp. 1–30.
27 B.-j. Yang, W. Luo, Q. Liao, J.-y. Zhu, M. Gan, X.-d. Liu and G.-z. Qiu, Photogenerated-hole scavenger for enhancing photocatalytic chalcopyrite bioleaching, *Trans. Nonferrous Met. Soc. China*, 2020, **30**, 200–211.
28 M. Long, J. Brame, F. Qin, J. Bao, Q. Li and P. J. J. Alvarez, Phosphate Changes Effect of Humic Acids on TiO2 Photocatalysis: From Inhibition to Mitigation of Electron–Hole Recombination, *Environ. Sci. Technol.*, 2017, **51**, 514–521.
29 L. C. Garzón and F. Martínez, Temperature Dependence of Solubility for Ibuprofen in Some Organic and Aqueous Solvents, *J. Solution Chem.*, 2004, **33**, 1379–1395.
30 S. H. Yalkowsky, Y. He and P. Jain, *Handbook of Aqueous Solubility Data*, CRC Press, Boca Raton, FL, 2010.
31 C. Gomes Silva, R. Juárez, T. Marino, R. Molinari and H. Garcia, Influence of Excitation Wavelength (UV or Visible Light) on the Photocatalytic Activity of Titania Containing Gold Nanoparticles for the Generation of Hydrogen or Oxygen from Water, *J. Am. Chem. Soc.*, 2011, **133**, 595–602.
32 L. Liu, X. Zhang, L. Yang, L. Ren, D. Wang and J. Ye, Metal nanoparticles induced photocatalysis, *Natl. Sci. Rev.*, 2017, **4**, 761–780.
33 X. Chen, L. Liu, Y. Yu Peter and S. Mao Samuel, Increasing Solar Absorption for Photocatalysis with Black Hydrogenated Titanium Dioxide Nanocrystals, *Science*, 2011, **331**, 746–750.
34 L. Lin, W. Jiang, M. Bechelany, M. Nasr, J. Jarvis, T. Schaub, R. R. Sapkota, P. Miele, H. Wang and P. Xu, Adsorption and photocatalytic oxidation of ibuprofen using nanocomposites of TiO2 nanofibers combined with BN nanosheets: Degradation products and mechanisms, *Chemosphere*, 2019, **220**, 921–929.
35 J. Madhavan, F. Grieser and M. Ashokkumar, Combined advanced oxidation processes for the synergistic degradation of ibuprofen in aqueous environments, *J. Hazard. Mater.*, 2010, **178**, 202–208.

 